Virus Research 294 (2021) 198290

Contents lists available at ScienceDirect

Virus Research

journal homepage: www.elsevier.com/locate/virusres

Antiviral activity of glycyrrhizic acid conjugates with amino acid esters against Zika virus

Lidia A. Baltina [a,**], Mann-Jen Hour [b,1], Ya-Chi Liu [c,d], Young-Sheng Chang [c,d], Su-Hua Huang [e], Hsueh-Chou Lai [f], Rimma M. Kondratenko [g], Svetlana F. Petrova [a], Marat S. Yunusov [a], Cheng-Wen Lin [c,d,e,*]

[a] Ufa Institute of Chemistry, Ufa Federal Research Centre of RAS, Ufa, 450054, Russian Federation
[b] School of Pharmacy, China Medical University, Taichung, 40402, Taiwan
[c] Department of Medical Laboratory Science and Biotechnology, China Medical University, Taichung, 40402, Taiwan
[d] Graduate Institute of Biomedical Sciences, College of Medicine, China Medical University, Taichung, 40402, Taiwan
[e] Department of Biotechnology, Asia University, Taichung 41354, Taiwan
[f] Division of Hepato-gastroenterology, Department of Internal Medicine, China Medical University Hospital, Taichung, 40447, Taiwan
[g] Bashkir State Medical University, Lenin's Street, Ufa, Russian Federation

ARTICLE INFO

Keywords:
Glycyrrhizic acid
Amino acid ester
Zika virus
Antiviral activity
Molecular modeling

ABSTRACT

Zika virus (ZIKV) is a new pathogenic flavivirus transmitted by mosquitoes *Aedes spp*. ZIKV infection is accompanied by serious neurological complications and is especially dangerous for pregnant women, in which it can lead to congenital malformations of the fetus and microcephaly in neonates. Currently, there are no licensed vaccines or specific post-infectious therapies for ZIKV infection. This report is devoted to the study of glycyrrhizic acid (GL) derivatives as ZIKV inhibitors. The inhibitory assays on the cytopathic effect (CPE) and viral infectivity of ZIKV in three different human cell lines revealed that the conjugation of GL with amino acids and their esters (methyl, ethyl) is influenced by the antiviral activity of the compounds. GL conjugates with Glu(OMe)-OMe **11**, Glu(OH)-OMe **12**, Asp(OMe)-OMe **13**, TyrOMe **14**, LeuOEt **15**, and PheOEt **16** with free COOH groups in the triterpene moiety were active against ZIKV. The most active compounds **13** and **14** have IC50 values of 0.23 μM and 0.09 μM against low doses (MOI = 0.05) of ZIKV strain PRVABC59, 1.20 μM and 0.74 μM against high doses (MOI = 10) of ZIKV strain Natal RGN single-round infectious particles, respectively. The lead compound was **14** with a high selectivity index (SI < 500). Compound **13** showed a higher inhibitory effect on the early stage (entry) of ZIKV replication than compound **14**, and was less potent than compound **14** at the post-entry stage, consistent with the docking models. Compounds **13** and **14** also had a strong interaction with the active site pocket of NS5 MTase. Compounds **13** and **14** are recommended for expanded antiviral studies against ZIKV infection.

1. Introduction

A new viral threat to humanity was announced in February 2016 by the World Health Organization (WHO) caused by the Zika virus (ZIKV), which is spread by mosquitoes *Aedes spp.*, and is related to yellow fever, Japanese encephalitis, and dengue viruses (World Health Organization, 2016; Weaver et al., 2016). ZIKV is a new pathogenic flavivirus belonging to the family Flaviviridae of the genus *Flavivirus* (Zanluca and Duarte dos Santos, 2016; Ye et al., 2016). ZIKV virions contain a single-stranded genomic RNA with one open reading frame, which is translated into a single polyprotein, giving rise to three structural proteins forming a virion (capsid, pre-membrane/membrane, and envelope) and seven nonstructural proteins (NS1, NS2a, NS2b, NS3, NS4a, NS4b, NS5) (Zanluca and Duarte dos Santos, 2016). Among these

* Corresponding author at: Department of Medical Laboratory Science and Biotechnology, China Medical University, 91, Hsueh-Shin Rd., Taichung, 40402, Taiwan.
** Corresponding author at: Ufa Institute of Chemistry, Ufa Federal Research Centre of RAS, 71, Prospect Oktyabrya, Ufa, 450054, Russian Federation.
E-mail addresses: baltina@anrb.ru (L.A. Baltina), cwlin@mail.cmu.edu.tw (C.-W. Lin).
[1] Co-first author.

https://doi.org/10.1016/j.virusres.2020.198290
Received 24 March 2020; Received in revised form 15 December 2020; Accepted 25 December 2020
Available online 31 December 2020

proteins, NS3 has protease and helicase activity, while NS5 contains methyltransferase and RNA-dependent RNA polymerase. Thus, NS3 and NS5 are targets for the development of anti-ZIKV agents (Li et al., 2017; Yang et al., 2018; Zhang et al., 2017; Godoy et al., 2017). In the first 60 years after its discovery (1947), the geographical locations of ZIKV were confirmed, with cases of human infection occurring sporadically only in Africa and Asia (Musso et al., 2014; Chang et al., 2016). In 2007, the first major outbreak of infection in Micronesia was recorded, affecting over 70 % of the population (Weaver et al., 2016). Subsequently, ZIKV infections were registered in Cambodia, the Philippines, and Thailand in 2010–2014 (Zanluca and Duarte dos Santos, 2016). Another large Zika epidemic, with 500,000–1,500,000 cases, occurred in Brazil at the end of 2015. From Brazil, ZIKV has spread to other countries of the American continent. Thus, in 2015–2016, Zika cases were reported in 69 countries and territories (Petersen et al., 2016). In 2018, an outbreak of ZIKV infection was recorded in India and Southeast Asia (Musso et al., 2019; Grubaugh et al., 2019). Most ZIKV-infected (80 %) people are asymptomatic carriers of ZIKV, and the clinical syndromes of ZIKV infection include Zika fever, similar to dengue fever, and congenital Zika syndrome (Musso et al., 2014; Chan et al., 2016). ZIKV infection is accompanied by serious neurological complications, such as Guillain-Barre Syndrome (Brasil et al., 2016). ZIKV infection is especially dangerous for pregnant women, in which it can lead to congenital malformations of the fetus and microcephaly in neonates (Weaver et al., 2016). It has now been established that ZIKV can be transmitted perinatally during childbirth through breast milk. The virus has also been detected in semen and can be transmitted through blood banks (Chan et al., 2016; Mlakar et al., 2016). Currently, there are no licensed vaccines or specific post-infectious therapy for ZIKV infection, and existing treatments are only supportive (Musso et al., 2019; Kim, 2019).

One of the natural compounds used as a basis for the creation of new antivirals is glycyrrhizic acid (GL) (**1**), the main bioactive triterpene glycoside of licorice roots (*Glycyrrhiza glabra* L., *GL. uralensis Fisher*) (Pompei et al., 2009; Baltina et al., 2009). GL and its derivatives inhibit some DNA and RNA viruses, including hepatitis A, B, and C viruses (HAV, HBV, and HCV) (Crance et al., 1994; Baltina et al., 2009; Matsumoto et al., 2013), human immunodeficiency virus-1 (HIV-1) (De Clerq, 2000), SARS coronaviruses (SARS-CoV) (Hoever et al., 2005), herpes simplex virus 1 (HSV-1) (Sekizawa et al., 2001), Epstein-Barr virus (EBV) (Lin et al., 2008), influenza A/H5N1 (Michaelis et al., 2010), and H1N1 viruses (IAV) (Baltina et al., 2015). GL is used for the treatment of chronic hepatitis and allergies (compound glycyrrhizin injection, compound glycyrrhizin injection tablets) (JMP F0115). Recently, we discovered the inhibitory activity of GL and its derivatives against dengue virus type 2 (DENV2) (Baltina et al., 2019). Several studies have demonstrated that GL and its derivatives impede early steps of the viral lifecycle, including virus entry (SARS-CoV) (Hoever et al., 2005), fusion (HIV-1) (De Clerq, 2000), penetration (HAV and EBV) (Crance et al., 1994; Lin et al., 2008), and endocytosis (IAV) (Michaelis et al., 2010; Baltina et al., 2015). Others show that GL and its derivatives effectively affect post-entry steps, such as genome replication (HSV-1, EBV, and HIV) (Sekizawa et al., 2001; Lin et al., 2008; De Clerq, 2000) and virus release (HCV) (Matsumoto et al., 2013). Moreover, GL and its derivatives with a low toxicity and a high bioavailability (Tolstikov et al., 2007) initiate gamma interferon production *in vitro* and *in vivo* (Pompei et al., 2009; Baltina et al., 2009; Matsumoto et al., 2013). However, the direct antiviral mechanisms of GL and its derivatives have yet to be defined.

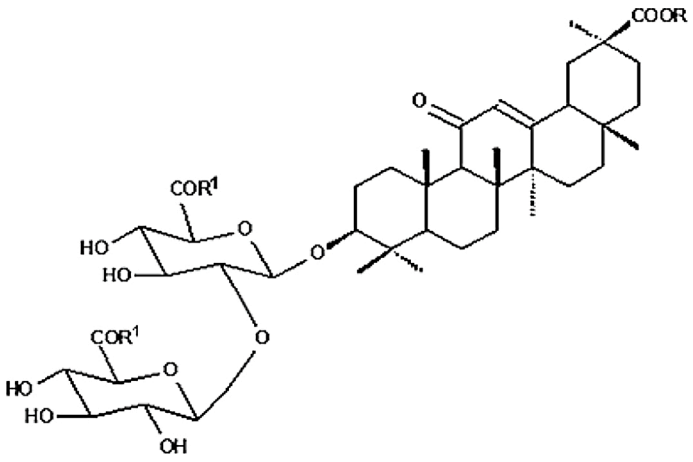

1 R = R^1 = OH

2 R = R^1 = Val-OMe

3 R = R^1 = D-ValOMe

4 R = R^1 = LeuOMe

5 R = R^1 = D-LeuOMe

6 R = R^1 = MetOMe

7 R = R^1 = PheOMe

8 R = R^1 = D-PheOMe

9 R = R^1 = TyrOMe

10 R = R^1 = D-TrpOMe

11 R = OH, R^1 = Glu(OMe)-OMe

12 R = OH, R^1 = Glu(OMe)-OH

13 R = OH, R^1 = Asp(OMe)-OMe

14 R = OH, R^1 = TyrOMe

15 R = OH, R^1 = LeuOEt

16 R = OH, R^1 = PheOEt

17 R = OH, R^1 = Gly-PheOEt

18 R = OH, R^1 = Leu

19 R = OH, R^1 = Met

20 R = OH, R^1 = Lys(Z)

21 R = OH, R^1 = TyrOH

Fig. 1. Structure of GL and derivatives **(compounds 2-21).** The GL derivatives contained three residues of L- and D-amino acids methyl esters (compounds **2-10**, group I), two amino acid methyl ester residues (compounds **11-14**, group II), two amino acid ethyl ester residues (compounds **15-17**, group III), and two free amino acid residues (compounds **18-21**, group IV) at the carbohydrate part of the glycosides.

The aim of this study was to examine the antiviral activity and mechanism of GL and its derivatives against ZIKV infection *in vitro*. Herein, 20 G L derivatives (compounds **2-21**) were divided into four groups (Fig. 1). Group I (compounds **2–10**) is the conjugate of GL with three amino acid methyl ester residues. Group II (compounds **11-14**) is represented by GL conjugates containing two amino acid methyl ester residues in the sugar part. Group III (compounds **15-17**) includes GL conjugates with two amino acid ethyl ester residues in the carbohydrate chain. Group IV (compounds **18-21**) presented by GL conjugates containing free amino acid residues in the sugar part. The compounds of groups II—IV have a free COOH group (at the C20 position) in the triterpene core of the molecule. For these four groups of GL derivatives, their antiviral activity against ZIKV strain PRVABC59 and Natal RGN (Lanciotti et al., 2016; Lu et al., 2019) was analyzed in different types of human cell lines, and their antiviral mechanisms were elucidated using time-of-addition assays.

2. Materials and methods

2.1. Cells and viruses

BHK-21 cells were used to amplify the ZIKV strain PRVABC59 for the production of viral stock (Lanciotti et al., 2016). The ZIKV strain Natal RGN that detected in the brain tissue of a microcephalic fetus was rescued as single-round infectious particles (SRIPs) using synthetic and reverse genetic technologies in our laboratory (Lu et al., 2019). Human glioma and astrocytoma SF268, human lung epithelial A549 cells, and TE671 cells were used for testing the anti-ZIKV activities and mechanisms of the GL derivatives. These cell lines were grown in MEM supplemented with 5 % fetal bovine serum (FBS), glutamine, pyruvate, and penicillin/streptomycin.

2.2. Chemicals

Commercially available N-hydroxybenzotriazole, N-hydroxysuccinimide, N,N'-diciclohexylcarbodiimid, 1-ethyl-3-(3-dimethylaminopropyl)carbodiimide-hydrochloride (Sigma-Aldrich), L- and D-amino acid methyl, and ethyl ester hydrochlorides (Sigma-Aldrich) were used as reagents.

2.3. Synthesis of GL derivatives with amino acid esters

GL (96.0 % purity) was purchased from Beijing Qinwutian Medical Technology Co., Ltd. (China) as a basic compound and was produced from the commercially available mono-ammonium salt, as described by Kondratenko et al. (2001). The synthesis of GL derivatives **2–10** (Fig. 1), containing three residues of L- and D-amino acid methyl esters, was performed using N-hydroxybenzotriazole (HOBt) and N,N'-diciclohexylcarbodiimid (DCC) or 1-ethyl-3-(3-dimethylaminopropyl)carbodiimid-hydrochloride (DEC), according to the protocols described in the Supplementary Material and previous studies (Baltina Jr et al., 2016; Fayrushina et al., 2017; Kondratenko et al., 2006; Baltina Jr et al., 2006, 2009; Baltina Jr et al., 2012, 2017). In brief, GL derivatives **11-17**, containing two methyl esters of amino acids Gly-PheOEt residues at the carbohydrate part of the glycosides, were prepared using N-hydroxysuccinimide (HOSu) and N,N'-dicyclohexylcarbodiimide (DCC) in different ratios of reagents and reaction conditions (Kondratenko et al., 2006; Baltina Jr et al., 2012). Compounds **15–17** were produced first. GL derivatives **18–20** were synthesized using tert-butyl esters of leucine, methionine, and ε-carbobenzoxy-lysine by the de-blocking of tert-butyl ester groups with CF_3COOH (Baltina Jr et al., 2006; Baltina Jr et al., 2006). Compound **18** was synthesized for the first time. The synthesis of the GL conjugate with tyrosine **21** is described in Baltina Jr et al. (2017). The analytical and spectral data of GL conjugates **2–14** and **19–21** were identical to the previously published data (Baltina Jr et al., 2016; Fayrushina et al., 2017; Kondratenko et al., 2006; Baltina Jr et al., 2006, 2009; Baltina Jr et al., 2012, 2017). All target compounds were purified by column chromatography on silica gel. The structures of new compounds **15–18** were confirmed by IR and ^{13}C NMR spectra and elemental analysis. The ^{13}C NMR spectra were recorded using a Bruker AVANCE-III pulse spectrometer at 500.30 MHz (^{1}H) and 125.75 MHz (^{13}C) in CD_3OD or DMSO-d_6. The IR spectra were recorded on a Prestige-21 spectrophotometer (Shimadzu) (Supplementary Material). Optical rotation was measured on a Perkin-Elmer 341 MC digital polarimeter with a sodium lamp (D-line wavelength =589 nm). The purity of the compounds was controlled by thin-layer chromatography and high-pressure liquid chromatography and was $\geq$ 95 % (Supplemental Fig. 1).

2.4. MTT assay

The cytotoxicity of the GL derivatives to human glioma SF268 cells and human lung epithelial A549 cells was tested using the MTT assay (Baltina et al., 2019; Lien et al., 2018). SF268 cells (3×10^3 cells/well) or A549 cells (5×10^3 cells/well) in 96-well plates were treated with GL derivatives (0, 0.1, 10, 20, and 50 μM) for 96 h with medium containing 2% FBS before adding to the MTT solution for 4 h. The reduction ability of MTT to purple formazan, indicating cell viability, was evaluated using an ELISA reader with an absorbance of $OD_{570\text{-}630}$.

2.5. Antiviral assay with ZIKV strain PRVABC59

To analyze the inhibitory activity of GL and its derivatives **2-21**, SF268 and A549 cells were infected with ZIKV strain PRVABC59 (MOI of 0.05) and simultaneously treated with GL or its derivatives at concentrations of 0.1, 1, and 10 μM, respectively. After a 96 -h incubation period with media containing 2% FBS, the ZIKV-induced cytopathic effect in infected/treated cells was photographed under a microscope. The residual post-treatment ZIKV infectivity in treated cells was determined using immunofluorescence staining with rabbit anti-ZIKV-NS1 (GeneTex, Inc) and anti-rabbit IgG antibodies conjugated with AF555 (ThermoFisher). Infectivity was determined according to the ratio of NS1-positive cells to total nuclei stained with DAPI (4′,6-diamidino-2-phenylindole). The infectivity was represented as the ratio of ZIKV NS1-positive cells (red fluorescent signals) to total cells (blue fluorescent signals), according to the image analysis of stained cells using Image J software. The inhibitory activity against ZIKV infection was calculated as follows: [1 − (% of NS1-positive infected cells with the treatment / % of NS1-positive infected cells without the treatment)] × 100 %. Fifty percent (50 %) inhibitory concentration (IC_{50}) reducing the relative ZIKV infectivity by 50 % was calculated using a computer program, and the selectivity index (SI) derived from the ratio of CC_{50} to IC_{50}.

2.6. Antiviral assay with SRIPs of ZIKV strain Natal RGN

High dose (MOI = 10) of ZIKV strain Natal RGN SRIPs containing an EGFP reporter was prepared to infect human lung epithelial A549 cells in the presence or absence of GL derivatives. After 72 h of incubation, ZIKV-induced CPE and the fluorescence of SRIP-driven EGFP reporter in infected cells were photographed using an inverted fluorescence microscope. Then, the treated infected cells were lysed using the lytic reagent (Passive Lysis 5X buffer) (Promega), and each lysate per well was transferred into a 96-well plate. Finally, the relative green fluorescence intensity of the ZIKV SRIP-driven EGFP reporter in the cells was measured at an excitation wavelength of 485 nm and an emission wavelength of 535 nm using a SpectraMax® iD3 Multi-Mode Microplate Reader (Molecular Devices). The inhibitory activity against ZIKV infection was calculated as follows: [1 − (fluorescence intensity of treated infected cells / fluorescence intensity of untreated infected cells)] × 100 %. IC_{50} was calculated as described above.

2.7. Time-of-addition/removal assay

The time-of-addition/removal assays comprised two modes of co-treatment/removal and post-infection treatment/removal assays (Weng et al., 2019). In the entry stage mode, compounds **13** or **14** (0, 0.1, 1, and 10 μM) and ZIKV (MOI = 0.5) were simultaneously added into the SF268 cells, cultured for 2 h, and washed out. The treated/infected cells were further incubated for 18 h and executed by an immune fluorescent staining assay to determine the residual ZIKV infectivity. In the post-entry stage mode, compounds **13** or **14** were added to the infected cells 2 h after infection, treated for 2 h, and washed out. After an 18 -h incubation period, the treated/infected cells were evaluated for residual ZIKV infectivity using an immune fluorescent staining assay. The inhibitory activity of the GL derivatives on the entry and post-entry stages of ZIKV replication was determined based on the residual infectivity (a relative NS1 positive rate in treated/ infected cells) in both modes. Subsequently, the model for the pre-treatment of the cells with the active GL derivatives before viral inoculation was performed to examine the possible actions on viral attachment or interferon production. SF268 cells were pretreated with compound **13** or **14** (0, 0.1, 1, and 10 μM) for 2 h, washed with PBS, and then infected with ZIKV at an MOI of 0.5 for 2 h, and washed out. After an 18 -h incubation period, the residual ZIKV infectivity was determined, as described above.

2.8. Molecular docking

To model the interaction of the GL derivatives with possible ZIKV targets, the crystal structures of NS2B-NS3 protease (PDB ID: 5H6V), NS3 helicase (PDB ID: 5Y6N), NS5 MTase (PDB ID: 5GOZ), and NS5 RdRp (PDB ID: 5U04) were downloaded from the RCSB Protein Data Bank (http://www.rcsb.org/pdb) as GL targets (Li et al., 2017; Yang et al., 2018; Zhang et al., 2017; Godoy et al., 2017), and the CDOCK program within BIOVIA Discovery Studio v2019 was used for the molecular docking experiments. The active site residues of these targets are defined in previous reports (Li et al., 2017; Yang et al., 2018; Zhang et al., 2017; Godoy et al., 2017). The poses were pruned, the final optimization step was performed, and the best scoring poses were calculated.

2.9. Statistical analysis

All data obtained from three independent experiments were compared using one-way analysis of variance followed by Scheffe's post-hoc test using SPSS 12.0 (SPSS, Inc.). $P < 0.05$ was considered as a significant result.

3. Results

3.1. A comparison of anti-ZIKV ability among GL derivative groups

Initially, the cytotoxicity of the GL derivatives was evaluated using the MTT assay (Supplementary Figs. 2 and 3), which revealed that most GL derivatives were less toxic to human SF268 and A459 cells (CC_{50} > 50 μM). The antiviral ability of GL and its derivatives **2-21** at 10 μM against ZIKV was further tested using cytopathic effect (CPE) reduction and viral NS1-positive rate in SF268 cells (Table 1, Figs. 2 and 3). GL and its conjugates with Glu(OMe)-OMe **11**, Glu(OMe)-OH **12**, Asp(OMe)-OMe **13**, TyrOMe **14**, LeuOEt **15**, and PheOEt **16** at 10 μM exhibited high inhibitory activity in the ZIKV CPE test (+++) (Table 1). Thus, groups II and III of the GL derivatives had stronger inhibitory activities on ZIKV-induced CPE than the other groups (Figs. 2A and 3 A, top right side; Table 1). Infectivity was determined according to the ratio of NS1-positive cells to total nuclei, revealing that 10 μM of the most GL derivatives from groups II and III significantly reduced ZIKV infectivity greater than 70 % in SF268 cells (Table 1). Moreover, compound **13** showed >80 % inhibition of ZIKV infectivity in SF268 cells. Interestingly, the GL derivatives of group I were less active against ZIKV compared to groups II—IV, which demonstrated that the availability of free COOH in the triterpene part of the molecule was important to maintain antiviral activity.

Table 1
Antiviral activity of GL and its derivatives against Zika virus.

Compound	CPE reduction at 10 μM[a]	Infectivity inhibition (%) at 10 μM[b]	Antiviral activity (IC50, μM)[c]
1	+++	70.4 ± 0.2	0.77 ± 0.03
Group I derivatives			
2	–	–	ND
3	–	–	ND
4	++	64.7 ± 0.3	ND
5	+	52.7 ± 1.2	ND
6	++	66.2 ± 0.6	ND
7	–	–	ND
8	–	–	ND
9	–	–	ND
10	–	–	ND
Group II derivatives			
11	+++	73.0 ± 5.8	1.62 ± 0.41
12	+++	74.4 ± 1.9	1.07 ± 0.08
13	+++	83.3 ± 3.8	0.23 ± 0.04
14	+++	70.2 ± 0.5	0.09 ± 0.08
Group III derivatives			
15	+++	72.2 ± 0.5	1.47 ± 0.17
16	+++	70.6 ± 0.4	2.23 ± 0.72
17	++	62.0 ± 1.2	ND
Group IV derivatives			
18	++	68.0 ± 0.9	ND
19	++	66.5 ± 1.5	ND
20	++	64.3 ± 2.3	ND
21	+	54.4 ± 0.8	ND

[a] –, no effect; +, slight inhibition; ++, moderate inhibition; +++, strong inhibition.
[b] [1 − (% of NS1-positive infected cells with the treatment / % of NS1-positive infected cells without the treatment)] × 100 %.
[c] ND, not detected; mean ± standard deviation.

3.2. Antiviral activity of active GL derivatives against ZIKV

To evaluate the IC_{50} values against ZIKV, the GL derivatives of groups II and III were tested against ZIKV strain PRVABC59 at concentrations of 0, 0.1, 1, and 10 μM using CPE reduction and infectivity inhibition assays in infected SF268 cells (Figs. 2 and 3, Table 1). The GL derivatives of groups II and III showed a concentration-dependent reduction of CPE in ZIKV-infected cells. The immune fluorescent staining assay of treated/infected SF268 cells indicated that GL derivatives with Asp(OMe)-OMe **13** (IC_{50} = 0.23 ± 0.04 μM) and TyrOMe **14** (IC_{50} = 0.09 ± 0. 02 μM) showed a higher inhibitory activity than GL (IC_{50} = 0.77 ± 0.25 μM) against ZIKV infection (Table 1). Meanwhile, the human rhabdomyosarcoma cell line TE671 was used to examine the antiviral activity of compound **13** against ZIKV (Supplementary Fig. 4), in which compound **13** exhibited potent anti-ZIKV activity (IC_{50} = 0.43 μM). To test the antiviral activity of compounds 13 and 14 against the other ZIKV strains in the different cell lines, human lung epithelial A549 cells were co-treated with ZIKV strain Natal RGN SRIPs at an MOI of 10 and compound **13** or **14** at the indicated concentrations (Figs. 4 and 5). After a 72 -h incubation period, compounds **13** and **14** significantly reduced ZIKV strain Natal RGN-induced cytopathic effects and the green fluorescence of ZIKV SRIP-driven GFP reporter in treated/infected cells (Figs. 4 and 5). The relative fluorescence of the ZIKV SRIP-driven GFP reporter from each lysate of treated/infected cells indicated that the IC_{50} values of GL derivatives with Asp(OMe)-OMe **13** and TyrOMe **14** was

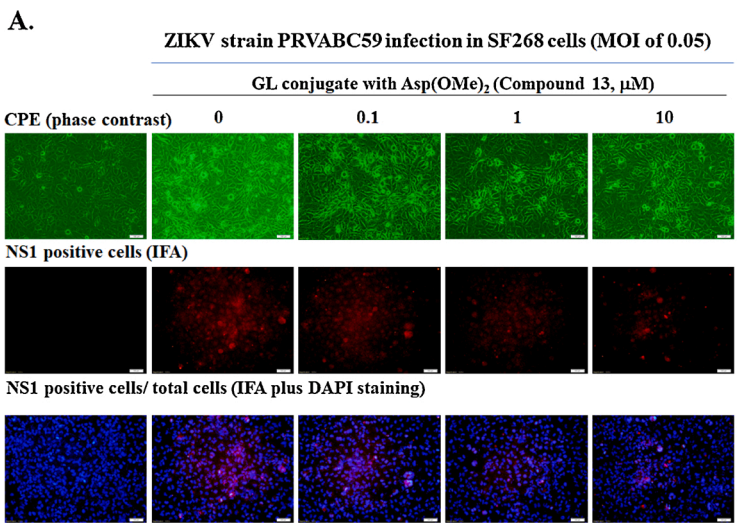

Fig. 2. Inhibitory effect of compound 13 on ZIKV strain PRVABC59-induced cytopathic effects and infectivity in SF268 cells. The cells were infected with ZIKV strain PRVABC59 at an MOI of 0.05 and immediately treated with compound **13** at the indicated concentrations. Images of ZIKV-induced cytopathic effects were photographed at 96 h post-infection by phase-contrast microscopy (A, top). Then, the treated/infected cells were assayed using immunofluorescence staining with anti-ZIKV NS1 antibodies and secondary antibodies conjugated with AF555 (A, middle). ZIKV infectivity was calculated as the ratio of NS1-positive cells to the total nuclei stained with DAPI (A, bottom; B). Infectivity inhibition was calculated for the decrease in the percentage of NS1-positive cells post-treatment. * $p < 0.05$; ** $p < 0.01$ compared with untreated infected cells. Scale bar, 100 μm.

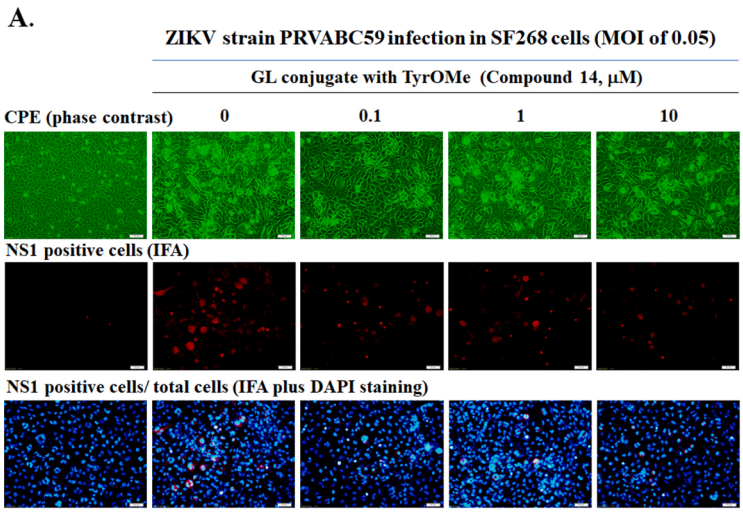

Fig. 3. Inhibitory effect of compound 14 on ZIKV strain PRVABC59-induced cytopathic effects and infectivity in SF268 cells. The cells were infected with ZIKV strain PRVABC59 at an MOI of 0.05 and immediately treated with compound **14** at the indicated concentrations. Images of ZIKV-induced cytopathic effects were photographed at 96 h post-infection by phase-contrast microscopy (A, top). Then, the treated/infected cells were assayed using immunofluorescence staining with anti-ZIKV NS1 antibodies and secondary antibodies conjugated with AF555 (A, middle). ZIKV infectivity was calculated as the ratio of NS1 positive cells to total nuclei stained with DAPI (A, bottom; B). Infectivity inhibition was calculated the decrease in the percentage of NS1-positive cells post-treatment. *** $p < 0.001$ compared with untreated infected cells. Scale bar, 100 μm.

1.20 ± 0.46 μM and 0.74 ± 0.02 μM, respectively, against a high dose of ZIKV strain Natal RGN SRIP infection in A549 cells. These results demonstrated that the group II GL derivatives, particular compounds **13** and **14**, had potent activity for diminishing ZIKV replication *via* a virus-strain and cell-type independent manner.

3.3. Anti-ZIKV action of GL derivatives *13* and *14*

To elucidate the antiviral mechanism of compounds **13** and **14**, a time-of-addition/removal assay was performed to examine the entry (during the first two hours of infection) and post-entry (2 h post-infection) stages of ZIKV replication, as well as pre-treatment before virus inoculation (Fig. 6 and 7). After an 18 -h incubation period (one round of viral replication), compounds **13** and **14** showed a stronger inhibition on the entry stage than the post-entry stage of ZIKV replication *in vitro* (Fig. 6). The IC_{50} values of compounds **13** and **14** on the entry stage of ZIKV replication *in vitro* were < 0.1 μM and 0.24 ± 0.05 μM, respectively. The time-of-addition assay also indicated that compound **14** was a higher inhibitory effect on the post-entry stage of ZIKV replication (IC_{50} = 1.31 ± 0.60 μM) than compound **13** (IC_{50} = 2.18 ± 0.39 μM) during ZIKV replication (Fig. 6). The model for the pre-treatment of the cells with compounds **13** and **14** 2 h before viral inoculation was used to analyze the effect on virus attachment and host antiviral factors (Fig. 7). Pre-treatment with compound **14** (IC_{50} = 7.85 ± 0.36 μM) had a higher inhibitory effect on viral infectivity than compound **13** (IC_{50} > 10 μM) (Fig. 7). The results revealed the difference between amino acid methyl ester residues ((Asp(OMe)-OMe **13**, and TyrOMe **14** in the sugar part of compounds **13** and **14** led to the alternation in the antiviral action, such as inhibiting the entry stage by compound **13** and blocking the post-entry state by compound **14**.

3.4. Interaction models of GL derivatives *13* and *14* with ZIKV NS5 MTase

To elucidate the relationship between the structure and the antiviral action of compounds **13** and **14**, molecular docking data showed that GL and its derivatives **13** and **14** fitted into the active site pocket of NS5 MTase (Fig. 8), but not to NS2B-NS3 protease, NS3 helicase, and NS5 RNA-dependent RNA polymerase. 5GOZ is a crystal structure of ZIKV NS5 MTase in complex with GTP and SAH, in which MTase has specific binding sites for both RNA and S-adenosylmethionine (SAM) and shares the binding site for GTP and RNA cap. There are three sites in ZIKV MTase: site 1 and site 2 are equivalent to the GTP/RNA cap-binding site, while site 3, equivalent to the RNA groove, is reported as an important pocket that is suitable for *in silico* high-throughput small-molecule screening. The 3D structures of GL and compounds **13** and **14**, were

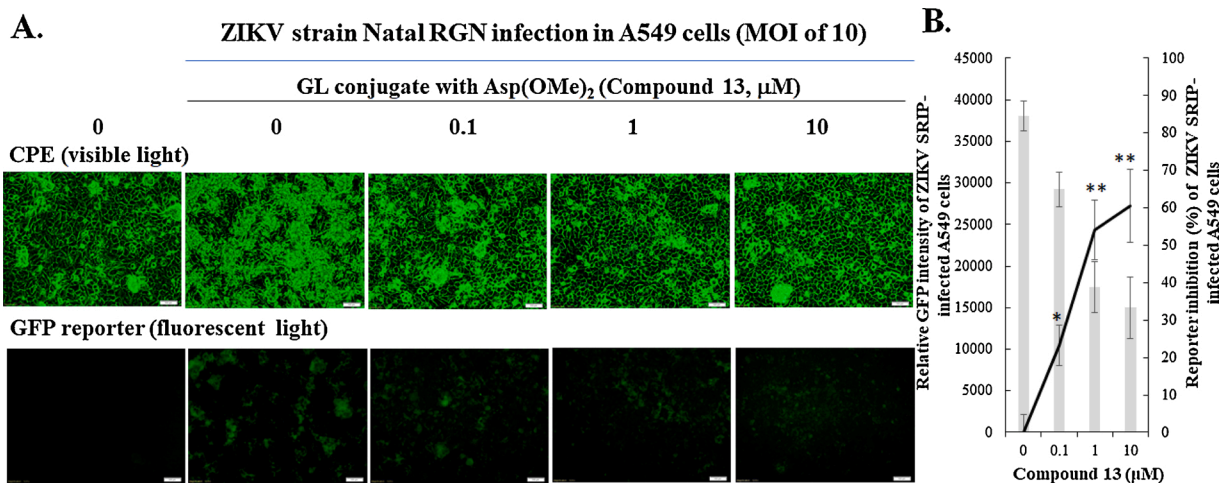

Fig. 4. Antiviral activity of compound 13 on ZIKV strain Natal RGN-induced cytopathic effects and infectivity in A549 cells. The cells were infected with ZIKV strain Natal RGN SRIPs at an MOI of 10 and immediately treated with compound **13** at the indicated concentrations. Images of ZIKV-induced cytopathic effects were photographed 72 h post-infection by phase-contrast microscopy (A, top). Then, the green fluorescence of ZIKV SRIP-driven GFP reporter in treated/infected cells was photographed using a fluorescence microscope (A, bottom). Relative fluorescence of ZIKV SRIP-driven GFP reporter from each lysate of treated/infected cells was measured using the SpectraMax® iD3 Multi-Mode Microplate Reader (B, left axis). Infectivity inhibition was estimated by the decrease in the fluorescence intensity in treated infected cells compared to that in untreated infected cells (B, right axis). * $p < 0.05$; ** $p < 0.01$ compared with untreated infected cells. Scale bar, 100 μm.

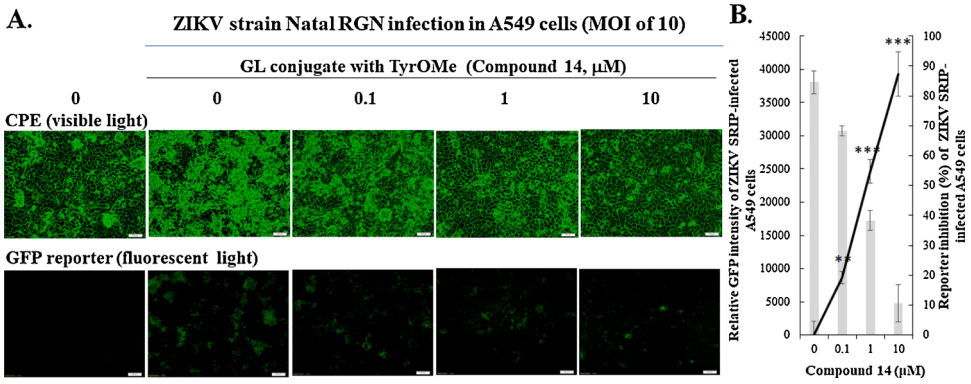

Fig. 5. Antiviral activity of compound 14 on ZIKV strain Natal RGN-induced cytopathic effects and infectivity in A549 cells. The cells were infected with ZIKV strain Natal RGN SRIPs at an MOI of 10 and immediately treated with compound **14** at the indicated concentrations. Images of ZIKV-induced cytopathic effects were photographed 72 h post-infection by phase-contrast microscopy (A, top). Then, the green fluorescence of ZIKV SRIP-driven GFP reporter in treated/infected cells was photographed using a fluorescence microscope (A, bottom). Relative fluorescence of ZIKV SRIP-driven GFP reporter from each lysate of treated/infected cells was measured using the SpectraMax® iD3 Multi-Mode Microplate Reader (B, left axis). Infectivity inhibition was estimated by the decrease in the fluorescence intensity in treated infected cells compared with that in untreated infected cells (B, right axis). * $p < 0.05$; ** $p < 0.01$ compared with untreated infected cells. Scale bar, 100 μm.

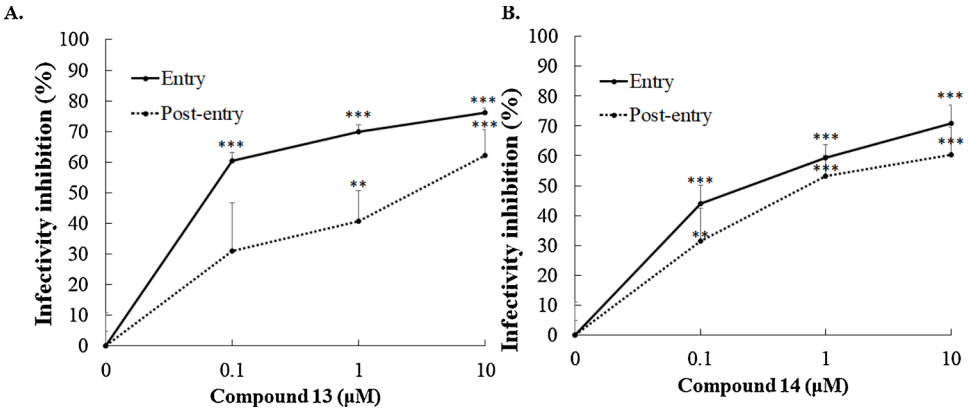

Fig. 6. Time-of-addition and removal assay for analyzing antiviral action of compounds 13 (A) and 14 (B) against ZIKV in SF268 cells. The cell monolayer was infected with ZIKV strain PRVABC59 (MOI = 0.5) and treated with the compounds simultaneously (the entry stage) or 2 -h post-infection (post-entry stage). After a 2 -h incubation period, the virus/compound mixture was removed; the cell monolayer was washed with PBS and cultured for 18 h and then subjected to immunofluorescence staining and DAPI. Infectivity inhibition was determined according to the decrease in the percentage of ZIKV NS1-positive cells. * $p < 0.05$; ** $p < 0.01$ compared with untreated infected cells.

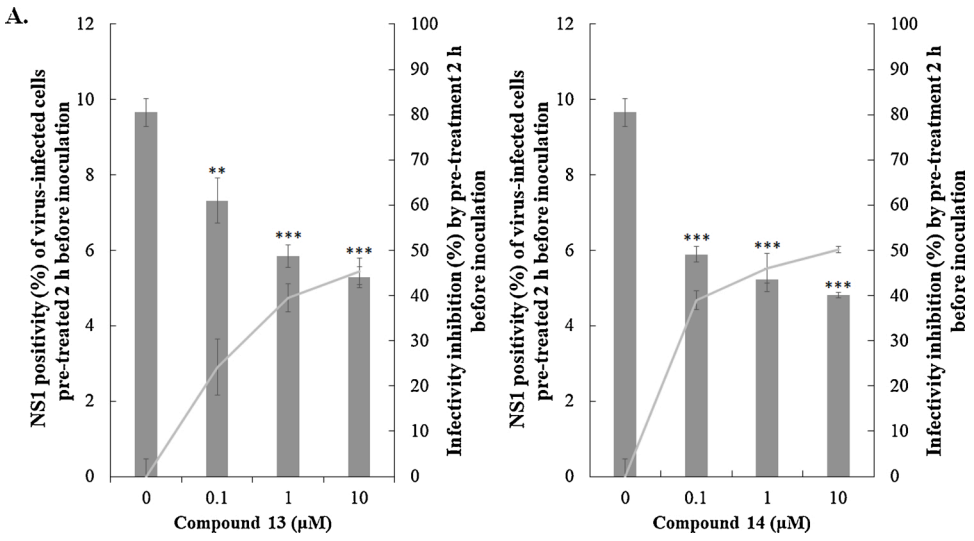

Fig. 7. Antiviral activity of compounds 13 and 14 *via* the pre-treatment of the cells before viral inoculation. The cell monolayer was pretreated with compound **13** or **14** for 2 h, washed with PBS, and then infected with ZIKV at an MOI of 0.5. After an 18 -h incubation period, the cell monolayer was assessed by immunofluorescence and DAPI staining. Infectivity inhibition was determined according to the decrease in the percentage of ZIKV NS1-positive cells. * $p < 0.05$; ** $p < 0.01$; *** $p < 0.001$ compared with untreated infected cells.

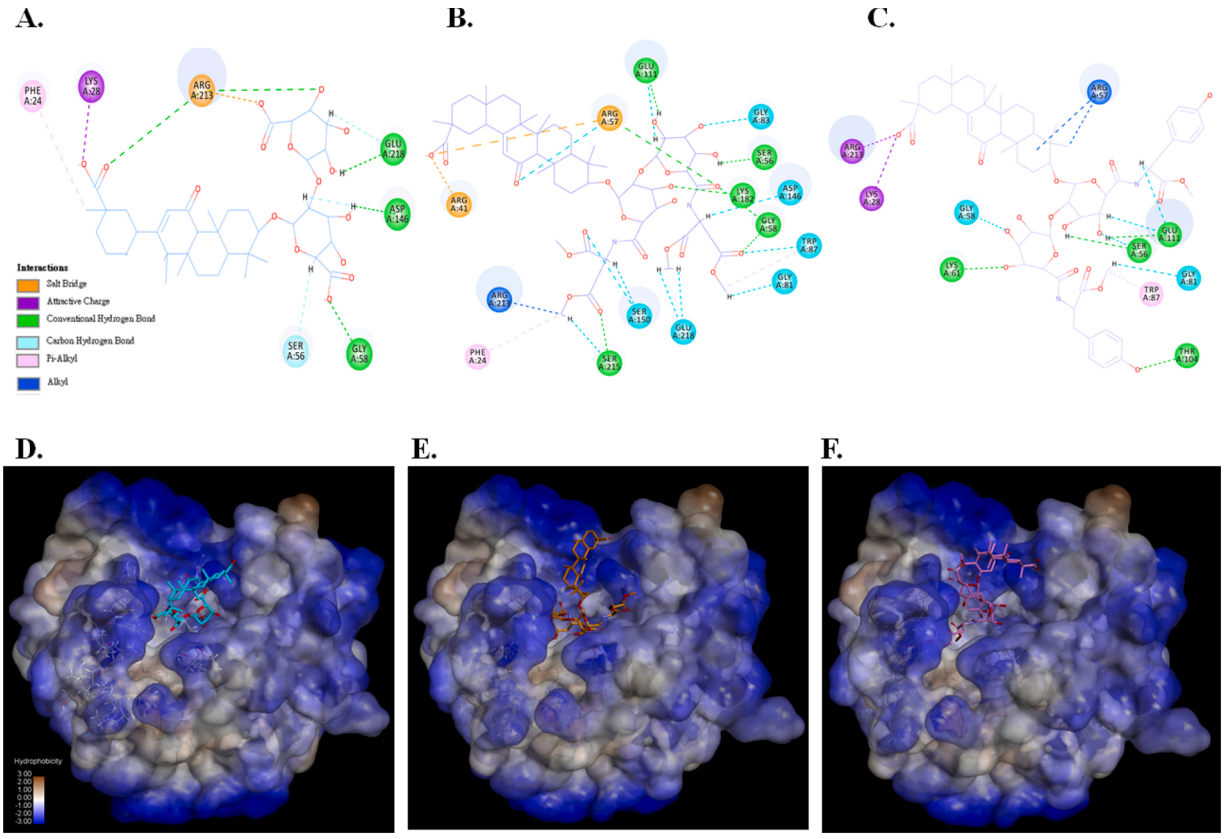

Fig. 8. Predicted interaction of GL and its derivatives 13 and 14 with ZIKV NS5 MTase. Two-dimensional model of the interaction of GL (A) and compounds **13** (B) and **14** (C) with ZIKV NS5 MTase (PDB ID: 5GOZ) using CDOCK program within BIOVIA Discovery Studio v2019. The hydrophobic reaction, salt bridges, hydrogen bonds, and (pi-) alkyl interactions were displayed in the docked models (A—C). Moreover, three-dimensional models of the interaction of GL (D) and compounds **13** (E) and **14** (F) with ZIKV NS5 MTase were established using the CDOCK program within BIOVIA Discovery Studio v2019.

processed by a minimization program first and docked into site 3 of 5GOZ with the CDOCK program. GL and compounds **13** and **14** were found to dock well with ZIKV MTase, respectively (Fig. 8). The negative CDOCKER energy for compounds **13** (-CDOCKER_Interaction Energy = 96.2502) and **14** (-CDOCKER_Interaction Energy = 88.4872) docking simulation with NS5 MTase was higher than that for GL (-CDOCKER_Interaction Energy = 86.6777). GL was stable *via* hydrogen bonding with Arg213, Glu218, Asp146, and Gly58, and showed attractive charge or hydrophobic interactions with Lys28, Phe24, Ser56, and Arg213 (Fig. 8A). Compound **13** was stable *via* hydrogen bonding with Ser56, Arg57, Gly58, Glu111, Lys182, and Ser215, and salt bridge or hydrophobic interactions with Phe24, Arg41, Arg57, Gly81, Gly83, Trp87, Asp146, Ser150, Arg213, and Glu218 (Fig. 8B). Compound **14** bound well *via* hydrogen bonds with Ser56, Lys61, and Glu111, and hydrophobic interactions with Lys28, Arg57, Gly58, Gly81, Trp87, and Arg213 (Fig. 8C). Thus, compounds **13** and **14** had a strong interaction

with the active site pocket of NS5 MTase, which is consistent with the significant effectiveness of compounds **13** and **14** in inhibiting the post-entry stage. The molecular model of GL and compounds **13** and **14** with NS5 MTase showed that the free COOH group in the triterpene part was crucial for forming salt bridges with positively charged residues (Lys28, Arg41, Arg57, and Arg213) within the active site pocket of NS5 MTase (Fig. 8). This finding was linked with the low antiviral activity of group I GL derivatives, containing amino acid residues in the triterpene moiety, which could influence the salt bridge formation and reduce their affinity. Importantly, Asp(OMe)-OMe and TyrOMe in the sugar part of compounds **13** and **14** had alkyl and pi-alkyl interactions with the aromatic residues (Phe24 and Trp87) within the active site pocket of NS5 MTase.

4. Discussion

To date, clinical trials of the Zika vaccine have been conducted in the USA, developed at the National Institute of Allergy and Infectious Diseases (NIAID) NIH (National Institute of Allergy and Infectious Diseases, 2017). Therefore, the relevance of creating new antivirals for the treatment of emerging infections with a global threat, such as ZIKV infection, is evident, and studies aimed at developing antiviral agents of this type are not only a priority in different countries but are also recommended by WHO. In the present study, the antiviral activity of GL and 20 derivatives was demonstrated against ZIKV strains PRVABC59 and Natal RGN. Compound **14** was the leading compound among the tested GL derivatives, exhibiting a higher SI (SI = CC50/IC50) of 67.6∼555.6 against low (MOI = 0.05) and high (MOI = 10) doses of ZIKV in SF268 and A549 cells, which was 8-fold greater than that for GL (Table 1, Figs. 1–5). Compound **13** was ranked as the second most active compound, showing a TI value of 41.7∼217 against low and high doses of ZIKV in two cell lines, which was 3-fold greater than that for GL (Table 1, Figs. 1–5). The GL derivatives in groups II and III were more active against ZIKV compared to those in groups I and IV, indicating that free amino acids in the sugar part of GL reduced the antiviral activity against ZIKV.

Time of drug addition and removal in experiments were used to analyze the antiviral mechanisms of compounds 13 and 14 against ZIKV (Figs. 6 and 7). Compound **13** exhibited a significant inhibitory effect on the entry stage, with IC_{50} values < 0.1 μM to the treatment of infected cells with a high dose of ZIKV 2 h post-infection after 18 h of incubation (one round of viral replication) (Fig. 6A). These results imply that compound **13** could be involved in blocking the interaction between the virus and the host cell receptors, thereby inducing the production of host antiviral factors. In addition, pre-treatment with compound **14** (IC_{50} = 7.85 ± 0.36 μM) and post-entry treatment by compound **14** (IC_{50} = 1.31 ± 0.60 μM) showed a greater antiviral ability than compound **13** (Figs. 6 and 7). The data revealed that compound **14** expressly interfered with the post-entry stages, including protein translation, genome replication, virus assembly, and virus release. However, real-time PCR assays indicated that compound **14** did not upregulate the expression of type I interferons in ZIKV-infected cells (data not shown). Thus, the structural difference between amino acid methyl ester residues (Asp(OMe)-OMe **13** and TyrOMe **14**) in the sugar part of GL derivatives might specifically regulate viral attachment stage (compound **13**) and post-entry (compound **14**) stages of ZIKV replication (Figs. 1,6 and 7). Our findings were similar to those of previous studies, wherein GL derivatives were found to affect virus entry (SARS-CoV) (Hoever et al., 2005), fusion (HIV-1) (De Clerq, 2000), penetration (HAV and EBV) (Crance et al., 1994; Lin et al., 2008), and endocytosis (IAV) (Michaelis et al., 2010; Baltina et al., 2015). Moreover, the GL derivatives could restrict genome replication (HSV-1, EBV, and HIV) (Sekizawa et al., 2001; Lin et al., 2008; De Clerq, 2000) and virus release (HCV) (Matsumoto et al., 2013). Therefore, the structural specificity of the GL derivatives provides a means with which to target different viral or host factors, showing unique features of antiviral mechanisms against many types of DNA and RNA viruses.

NS3, containing protease and helicase domains, and NS5, including methyltransferase (MTase) and RNA-dependent RNA polymerase (RdRp) domains, have been suggested as therapeutic targets during the post-entry stage of ZIKV replication (Li et al., 2017; Yang et al., 2018; Zhang et al., 2017; Godoy et al., 2017). The crystal structures of NS2B-NS3 protease (PDB ID: 5H6V), NS3 helicase (PDB ID: 5Y6N), NS5 MTase (PDB ID: 5GOZ), and NS5 RdRp (PDB ID: 5U04) were downloaded from the RCSB Protein Data Bank (http://www.rcsb.org/pdb) as drug targets, and the CDOCK program within BIOVIA Discovery Studio v2019 was used for the molecular docking experiments. This discovery may be associated with the low antiviral activity of the GL derivatives in group IV, in which the free amino acids in the sugar part had a lower affinity to NS5 MTase compared to the compounds of groups II and III (Fig. 8). The structure–antiviral activity study demonstrated that GL conjugates with free COOH groups in the triterpene moiety and amino acid methyl esters in the sugar part (compounds **13** and **14**) interacted well within the active site pocket of NS5 MTase *via* the formation of a salt bridge, hydrogen bonds, and (pi-)alkyl interactions between each other, exhibiting a high anti-ZIKV activity.

This study is the first report on the anti-ZIKV activity of GL and its derivatives, namely, conjugates with amino acids and their methyl/ethyl esters. GL was found to exert pronounced anti-ZIKV activity in the CPE test and infectivity inhibition. The structure–antiviral activity study demonstrated that the free COOH group in the triterpene part and two amino acid methyl esters in the sugar part of the GL derivatives played a critical role in improving the anti-ZIKV activity of GL, due to their involvement in its interaction with the active site pocket of NS5 MTase *via* the formation salt bridges, hydrogen bonds, and (pi-) alkyl interactions. Compounds **13** and **14** were the most active among the GL derivatives tested, exhibiting a powerful anti-ZIKV activity with multiple actions, including in the entry and post-entry stages. Thus, the advantages of using compounds **13** and **14** over GL make them suitable for expanded antiviral studies and for potential use as antiviral drugs to combat ZIKV infection.

Declaration of Competing Interest

The authors have no competing financial interests to declare.

Acknowledgments

This work was financially supported by the Russian Foundation for Basic Research (18-53-52004_MNT_a), the State Assignment (AAAA-A20-120012090029-0), China Medical University, Taiwan (CMU108-ASIA-11, CMU108-S-12, and CMU108-MF-42), and grants from the Ministry of Science and Technology, Taiwan (MOST107-2923-B-039-001-MY3). Experiments and data analysis were partly performed at the Medical Research Core Facilities Center, Office of Research & Development at China Medical University, Taiwan.

Appendix A. Supplementary data

Supplementary material related to this article can be found, in the online version, at doi:https://doi.org/10.1016/j.virusres.2020.198290.

References

Baltina Jr, L.A., Kondratenko, R.M., Baltina, L.A., Plyasunova, O.A., Galin, F.Z., Tolstikov, G.A., 2006. Synthesis of Glycyrrhizic acid conjugates containing L-lysine. Chem. Nat. Compd. 42, 543–548.

Baltina, L.A., Kondratenko, R.M., Baltina Jr., L.A., Plyasunova, O.A., Pokrovskyi, A.G., Tolstikov, G.A., 2009. Prospects for the creation of new antiviral drugs based on Glycyrrhizic acid and its derivatives. Pharm. Chem. J. 43, 539–548.

Baltina, L.A., Zarubaev, V.V., Baltina, L.A., Orshanskaya, I.A., Fairushina, A.I., Kiselev, O. I., Yunusov, M.S., 2015. Glycyrrhizic acid derivatives as influenza A/H1N1 virus inhibitors. Bioorg. Med. Chem. Lett. 25, 1742–1746.

Baltina, L.A., Tasi, Y.T., Huang, S.H., Lai, H.C., Baltina, L.A., Petrova, S.F., Yunusov, M. S., Lin, C.W., 2019. Glycyrrhizic acid derivatives as Dengue virus inhibitors. Bioorg. Med. Chem. Lett. 29, 126645.

Baltina Jr, L.A., Kondratenko, R.M., Baltina, L.A., Baschenko, N.Z., Plyasunova, O.A., 2009. Synthesis and biological activity of new glycyrrhizic acid conjugates with amino acids and dipeptides. Russ. J. Bioorg. Chem. 35, 510–517.

Baltina Jr, L.A., Chistoedova, E.S., Baltina, L.A., Kondratenko, R.M., Plyasunova, O.A., 2012. Synthesis and anti-HIV-1 activity of new conjugates of 18β- and 18α-Glycyrrhizic acids with aspartic acid esters. Chem. Nat. Compd. 48, 262–266.

Baltina Jr, L.A., Fairushina, A.I., Baltina, L.A., 2016. New methods of preparation of carboxy-protected amino acid conjugates of Glycyrrhizic acid. Russ. J. Gen. Chem. 86, 826–829.

Baltina Jr, L.A., Fairushina, A.I., Baltina, L.A., Eropkin, M.Y., Konovalova, N.I., Petrova, P.A., Eropkina, E.M., 2017. Synthesis and antiviral activity of Glycyrrhizic acid conjugates with aromatic amino acids. Chem. Nat. Compd. 53, 1096–1100.

Brasil, P., Sequeira, P.C., Freitas, A.D., Zogbi, H.E., Calvet, G.A., de Souza, R.V., Siqueira, A.M., de Mendonca, M.C.L., Mogueira, R.M.R., de Filippis, A.M.B., Solomon, T., 2016. Guillain-Barre syndrome associated with Zika virus infection. Lancet 10026, 1482.

Chan, J.F.W., Choi, G.K.Y., Yip, C.C.Y., Cheng, V.C.C., Yen, K.W., 2016. Zika fever and congenital Zika syndrome: an unexpected emerging arboviral disease. J. Infection 72, 507–524.

Chang, C., Ortiz, K., Ansari, A., Gershwin, M.E., 2016. The Zika outbreak of the 21st century. J. Autoimmunity 68, 1–13.

Crance, J.M., Lévêque, F., Biziagos, E., van Cuyck-Gandré, H., Jouan, A., Deloince, R., 1994. Studies on mechanism of action of glycyrrhizin against hepatitis A virus replication *in vitro*. Antiviral Res. 23, 63–76.

De Clerq, E., 2000. Current lead natural products for the chemotherapy of human immunodeficiency virus (HIV) infection. Med. Res. Rev. 20, 323–349.

Fayrushina, A.I., Baltina Jr, L.A., Baltina, L.A., Konovalova, N.I., Petrova, P.A., Eropkin, M.Y., 2017. Synthesis and antiviral activity of novel Glycyrrhizic acid conjugates with D-aminoacids. Russ. J. Bioorg. Chem. 43, 456–462.

Godoy, A.S., Lima, G.M., Oliveira, K.I., Torres, N.U., Maluf, F.V., Guido, R.V., Oliva, G., 2017. Crystal structure of Zika virus NS5 RNA-dependent RNA polymerase. Nat. Commun. 8, 14764.

Grubaugh, N.D., Ishtiaq, F., Setoh, Y.X., Ko, A.I., 2019. Misperceived risks of Zika-related microcephaly in India. Trends Microbiol. 27, 381–383.

Hoever, H., Baltina, L.A., Nichaelis, M., Kondratenko, R.M., Baltina, L.A., Tolstikov, G.A., Doerr, H.W., Cinatl, J., 2005. Antiviral activity of Glycyrrhizic acid derivatives against SARS-Coronavirus. J. Med. Chem. 48, 1256–1259.

Kim, K.S., 2019. Current challenges in the development of vaccines and drugs against emerging vector-borne diseases. Curr. Med. Chem. 26 (16), 2974-298.

Kondratenko, R.M., Baltina, L.A., Mustafina, S.R., Makarova, N.V., Nasyrov, K.M., Tolstikov, G.A., 2001. Crystalline Glycyrrhizic acid synthesized from commercial glycyrrham. Immunomodulant properties of high-purity Glycyrrhizic acid. Pharm. Chem. J. 35, 101–104.

Kondratenko, R.M., Baltina Jr, L.A., Baltina, L.A., Baschenko, N.Z., Tolstikov, G.A., 2006. Synthesis and immunomodulating activity of new glycopeptides of Glycyrrhizic acid containing residues of L-Glutamic acid. Russ. J. Bioorg. Chem. 32, 660–666.

Li, Y., Zhang, Z., Phoo, W.W., Loh, Y.R., Wang, W., Liu, S., Chen, M.W., Hung, A.W., Keller, T.H., Luo, D., Kang, C., 2017. Structural dynamics of zika virus NS2B-NS3 protease binding to dipeptide inhibitors. Structure 25 (8), 1242–1250.

Lien, J.C., Wang, C.Y., Lai, H.C., Lu, C.Y., Lin, Y.F., Gao, G.Y., Chen, K.C., Huang, A.C., Huang, S.H., Lin, C.W., 2018. Structure analysis and antiviral activity of CW-33 analogues against Japanese encephalitis virus. Sci. Rep. 8, 16595.

Lin, J.C., Cherng, J.M., Hung, M.S., Baltina, L.A., Baltina, L.A., Kondratenko, R.M., 2008. Inhibitory effects of some derivatives of Glycyrrhizic acid against Epstein-Barr virus infection: structure-activity relationships. Antiviral Res. 79, 6–11.

Lu, C.Y., Lin, C.S., Lai, H.C., Yu, Y.W., Liao, C.Y., Su, W.C., Ko, B.H., Chang, Y.S., Huang, S.H., Lin, C.W., 2019. The rescue and characterization of recombinant, Microcephaly-Associated Zika Viruses as single-round infectious particles. Viruses 11 (11), 1005.

Matsumoto, Y., Matsuura, T., Aoyagi, H., Matsuda, M., Hmwe, S.S., Date, T., Watanabe, N., Watashi, K., Suzuki, R., Ichinose, S., Wake, K., Suzuki, T., Miyamura, T., Wakita, T., Aizaki, H., 2013. Antiviral activity of Glycyrrhizin against hepatitis C virus *in vitro*. PLoS One 8, 1–10.

Michaelis, M., Geiler, J., Naczk, P., Sithisarn, P., Ogbomo, H., Altenbrandt, B., Leutz, A., Doerr, H.W., Cinatl Jr, J., 2010. Glycyrrhizin inhibits highly pathogenic H5N1 influenza A virus-induced pro-inflammatory cytokine and chemokine expression in human macrophages. Med. Microbiol. Immunol. 199, 291–297.

Mlakar, J., Korva, M., Tul, N., Popović, M., Poljšak-Prijatelj, M., Mraz, J., Kolenc, M., Resman Rus, K., Vesnaver Vipotnik, T., Fabjan Vodušek, V., Vizjak, A., Pižem, J., Petrovec, M., Avšič Županc, T., 2016. Zika virus associated with microcephaly. N. Engl. J. Med. 374, 951–958.

Musso, D., Nilles, E.J., Cao-Lormeau, V.M., 2014. Rapid spread of emerging Zika virus in the Pacific area. Clin. Microbiol. Infect. 20, O595–O596.

Musso, D., Ko, A.I., Baud, D., 2019. Zika virus infection – after the pandemic. N. Engl. J. Med. 381, 1444–1457.

National Institute of Allergy and Infectious Diseases (NIAID), 2017. Phase 2 Zika Vaccine Trial Begins in U.S., Central and South America. http://www.nih.gov/news-events/news-releases/phase-2-zika-vaccine-trial-begins-us-central-south-america.

Petersen, E., Wilson, M.E., Touch, S., McCloskey, B., Mwaba, P., Bates, M., Dar, O., Mattes, F., Kidd, M., Ippolito, G., Azhar, E.I., Zumla, A., 2016. Rapid spread of Zika virus in the Americas – implications for public health preparedness for mass gatherings at the 2016 Brazil Olympic Games. Int. J. Infect. Dis. 44, 11–15.

Pompei, R., Laconi, S., Ingianni, A., 2009. Antiviral properties of Glycyrrhizic acid and its semisynthetic derivatives. Mini-Rev Med. Chem. 9, 996–1001.

Sekizawa, T., Yanagi, K., Itoyama, Y., 2001. Glycyrrhizin increases survival of mice with herpes simplex encephalitis. Acta Virol. 45, 51–54.

Tolstikov, G.A., Baltina, L.A., Grankina, V.P., Kondratenko, R.M., Tolstikova, T.G., 2007. Licorice: Biodiversity, Chemistry, Medical Applications. Academic Publishing House "Geo", Novosibirsk, p. 311.

Weaver, S.C., Costa, F., Garcia-Blanco, M.A., Ko, A.I., Ribeiro, G.S., Saade, G., Shi, P.Y., Vasilakis, N., 2016. Zika virus: history, emergence, biology, and prospects for control. Antiviral Res. 130, 69–80.

Weng, J.R., Lin, C.S., Lai, H.C., Lin, Y.P., Wang, C.Y., Tsai, Y.C., Wu, K.C., Huang, S.H., Lin, C.W., 2019. Antiviral activity of Sambucus formosana Nakai ethanol extract and related phenolic acid constituents against human coronavirus NL63. Virus Res. 273, 197767.

World Health Organization, 2016. Zika Virus and Complications: Public Health Emergency of International Concern. World Heal. Organ. –Program. http://www.who.int/emergencies/zika-virus/en/.

Yang, X., Chen, C., Tian, H., Chi, H., Mu, Z., Zhang, T., Yang, K., Zhao, Q., Liu, X., Wang, Z., Ji, X., Yang, H., 2018. Mechanism of ATP hydrolysis by the Zika virus helicase. FASEB J. 32 (10), 5250–5257.

Ye, Q., Liu, Z.Y., Han, J.F., Jiang, T., Li, X.F., Qin, C.F., 2016. Genomic characterization and phylogenetic analysis of Zika virus. Infect. Genet. Evol. 43, 43–49.

Zanluca, C., Duarte dos Santos, C.D., 2016. Zika virus – an overview. Microbes Infect. 18, 295–301.

Zhang, C., Feng, T., Cheng, J., Li, Y., Yin, X., Zeng, W., Jin, X., Li, Y., Guo, F., Jin, T., 2017. Structure of the NS5 methyltransferase from Zika virus and implications in inhibitor design. Biochem. Biophys. Res. Commun. 492 (4), 624–630.